Proc. Natl. Acad. Sci. USA
Vol. 94, pp. 2981–2986, April 1997
Biochemistry

Mössbauer studies of alkane ω-hydroxylase: Evidence for a diiron cluster in an integral-membrane enzyme

(nonheme/oxygenase/desaturase/binuclear iron/cytochrome P450)

JOHN SHANKLIN*†, CATALINA ACHIM‡, HERMANN SCHMIDT*, BRIAN G. FOX§, AND ECKARD MÜNCK†‡

*Department of Biology, Brookhaven National Laboratory, Upton, NY 11973; ‡Department of Chemistry, Carnegie Mellon University, Pittsburgh PA 15213; and §Institute for Enzyme Research, University of Wisconsin, Madison, WI 53705

Communicated by JoAnne Stubbe, Massachusetts Institute of Technology, Cambridge, MA, January 18, 1997 (received for review October 25, 1996)

ABSTRACT **The gene encoding the alkane ω-hydroxylase (AlkB; EC 1.14.15.3) from *Pseudomonas oleovorans* was expressed in *Escherichia coli*. The integral-membrane protein was purified as nearly homogeneous protein vesicles by differential ultracentrifugation and HPLC cation exchange chromatography without the detergent solubilization normally required for membrane proteins. Purified AlkB had specific activity of up to 5 units/mg for octane-dependent NADPH consumption. Mössbauer studies of AlkB showed that it contains an exchange-coupled dinuclear iron cluster of the type found in soluble diiron proteins such as hemerythrin, ribonucleotide reductase, methane monooxygenase, stearoyl-acyl carrier protein (ACP) Δ^9 desaturase, rubrerythrin, and purple acid phosphatase. In the as-isolated enzyme, the cluster contains an antiferromagnetically coupled pair of high-spin Fe(III) sites, with an occupancy of up to 0.9 cluster per AlkB. The diferric cluster could be reduced by sodium dithionite, and the diferrous state was found to be stable in air. When both O_2 and substrate (octane) were added, however, the diferrous cluster was quantitatively reoxidized, proving that the diiron cluster occupies the active site. Mössbauer data on reduced AlkB are consistent with a cluster coordination rich in nitrogen-containing ligands. New sequence analyses indicate that at least 11 nonheme integral-membrane enzymes, including AlkB, contain the 8-histidine motif required for catalytic activity in stearoyl-CoA desaturase. Based on our Mössbauer studies of AlkB, we propose that the integral-membrane enzymes in this family contain diiron clusters. Because these enzymes catalyze a diverse range of oxygenation reactions, this proposal suggests a greatly expanded role for diiron clusters in O_2-activation biochemistry.**

The bacterial ω-hydroxylase is an enzyme system consisting of three protein components (1): a soluble NADH-rubredoxin reductase (2); a soluble rubredoxin (3); and an integral-membrane oxygenase referred to as ω- or alkane hydroxylase (AlkB) (4–6). In addition to the energetically demanding hydroxylation of unactivated aliphatic methyl groups, AlkB has been shown to catalyze a number of other characteristic reactions (7–9). These reactions are consistent with the involvement of high-valent, electrophilic catalytic intermediates comparable to those found in cytochrome P450 (10) and a number of other nonheme iron proteins (11). Previous optical and biochemical studies of AlkB have shown that the presence of nonheme iron was essential for catalysis, and that ≈1 mol of iron was present per mol of partially purified protein (5). However, due to problems inherent to working with membrane proteins, further structural characterization of the AlkB active site has not been reported.

Recently, we suggested that AlkB, the related bacterial xylene monooxygenase, and a large class of integral-membrane fatty acid desaturases, constitute a structurally related protein family (12). By using the rat stearoyl-CoA desaturase gene to complement a yeast unsaturated fatty acid auxotroph, we showed by mutational analysis that eight His residues were all essential for catalytic function (12). A combination of *alkB*-reporter gene fusion (13) and hydropathy analyses further suggested that these conserved His reside in equivalent hydrophilic domains on the cytoplasmic face of the membrane, supporting a model in which both the hydroxylases and desaturases share a common structural organization (12, 13). One interpretation of these results is that the conserved His residues act as ligands for the iron(s) present in the active site of this protein family.

Enzymes containing diiron clusters are capable of the oxidation of unactivated C–H bonds (11), such as the physiological reaction catalyzed by AlkB. Crystal structures of representatives from three distinct catalytic classes of soluble diiron enzymes, the aerobic component of ribonucleotide reductase (R2) (14), methane monooxygenase (MMO) (15), and stearoyl-acyl carrier protein (ACP) Δ^9 desaturase (Δ9D) (16), have revealed that these proteins share a common polypeptide fold. Although these diiron enzymes have no significant overall amino acid homology, they all contain an iron-binding motif consisting of two repeats of $Glu(Xaa)_2His$ (17, 18). Residues within the active site involved in hydrogen bonding and perhaps catalytic aspects may also be conserved (16, 18). The diiron-binding motif of the soluble proteins is absent from the integral-membrane hydroxylases and desaturases. Nevertheless, the numerous biochemical and catalytic similarities between the soluble and membrane classes prompted us to suggest that these membrane enzymes may also contain diiron centers (12).

In this report, we describe the expression of *Pseudomonas oleovorans* AlkB under the control of an inducible T7 polymerase in *Escherichia coli* and its purification. Analysis of the Mössbauer spectra of AlkB reveals a dinuclear iron cluster of the type found in diiron enzymes (17, 19–23). Single turnover experiments also monitored by Mössbauer spectroscopy demonstrate that both substrate (octane) and O_2 are required for the reoxidation of the diferrous center. When considered with an expanded identification of the eight-histidine motif in several new types of O_2-activating enzymes, our results suggest the presence of a diiron active site for a diverse family of integral-membrane enzymes.

MATERIALS AND METHODS

Materials. *P. oleovorans* was obtained from the American Type Culture Collection and grown on a minimal medium

The publication costs of this article were defrayed in part by page charge payment. This article must therefore be hereby marked "*advertisement*" in accordance with 18 U.S.C. §1734 solely to indicate this fact.

0027-8424/97/942981-6$2.00/0
PNAS is available online at **http://www.pnas.org**.

Abbreviations: AlkB, alkane ω-hydroxylase; Hr, hemerythrin; MMO, methane monooxygenase; R2, R2 subunit of ribonucleotide reductase; Δ9D, stearoyl-ACP Δ^9 desaturase; T4MO, toluene-4-monooxygenase; ACP, acyl carrier protein.

†To whom reprint requests should be addressed.

supplemented with octane (24). The OCT plasmid was isolated using a Wizard miniprep kit (Promega).

AlkB Expression. The alkane-hydroxylase gene, *alkB*, (GenBank accession no. J04618) (6) was amplified from the OCT plasmid by PCR using *Pfu* DNA polymerase (Stratagene) and the following primers: aattggagaTcTccaTatgcttgaga (coding) and gccgggctctgAgATctcacataac (noncoding) (lowercase characters are homologous to the *alkB* sequence; uppercase characters are mutations). These primers introduced *Bgl*II and *Nde*I sites into the 5′ flank and a *Bgl*II site into the 3′ flank of the 1206-bp coding region. The amplified product was restricted with *Nde*I and *Bgl*II and the fragment cloned into the corresponding *Nde*I and *Bam*HI sites in pET3a to make pAlkB-3a (25). Both strands of the insert were fully sequenced to confirm the presence of *AlkB* and ensure that secondary mutations had not been introduced. For expression, pAlkB-3a was introduced into *E. coli* BL21(DE3)pLysS and grown on 10 g/liter Bacto Tryptone, 5 g/liter NaCl, and 50 mg/liter ampicillin in baffled flasks shaken at 325 rpm at 37°C. Cells were grown to a density of 0.5 OD_{600}, at which time the medium was supplemented with 1.4 mg/liter of ^{57}Fe dissolved in a minimal volume of 6 M HCl (isotopic enrichment of ≈80%), and the temperature was lowered from 37°C to 30°C ($t = 0$ min). At 10 min, AlkB production was induced by addition of isopropyl-β-D-thiogalactopyranoside to 0.4 mM; at 30 min, rifampicin was added to a final concentration of 200 mg/liter; at 4 hr, the cells were collected by centrifugation at 16,000 × *g* for 6 min, washed once in 40 mM Tris·HCl, collected by centrifugation as before, and stored at −70°C.

AlkB Purification. All manipulations were carried out on ice or at 4°C unless otherwise specified. Cells (15 g) were resuspended in 50 ml of 50 mM Hepes (pH 8.0) containing 4 mM $MgCl_2$, 2 mM phenylmethylsulfonyl fluoride, 10 mg of DNase I, and 50 mg of catalase. The cell suspension was disrupted by single passage through a French pressure cell with a 70 MPa pressure drop. The resulting extract was clarified by centrifugation at 43,000 × *g* for 45 min. The supernatant fraction was divided among four 14 × 89 mm polyallomer SW41 centrifuge tubes (Beckman) and underlayed with 1.5 ml of 50 mM Hepes (pH 7.5) containing 40% (vol/vol) glycerol. The glycerol cushions were harvested after centrifugation at 285,000 × *g* for 90 min and diluted to 45 ml with 50 mM Hepes (pH 7.5) to which 5 ml of 5 M urea was added. The AlkB-enriched membrane fraction was collected by centrifugation at 240,000 × *g* for 1 hr, and resuspended in 12 ml of 25 mM Hepes (pH 7.5) containing 10% (vol/vol) ethylene glycol (buffer A) by sonication. The resuspended material was applied in three separate, equal volume portions at 1 ml/min to a 1 cm × 20 cm column of POROS 20CM (Perseptive Biosystems, Cambridge, MA) equilibrated with buffer A and eluted with a linear gradient of buffer A containing 0–600 mM NaCl at 4 ml/min over 38 min. Fractions enriched in AlkB were pooled and collected by centrifugation at 240,000 × *g* for 1 hr. The resulting pelleted fraction was resuspended by sonication in an approximately equal volume of buffer. The final enzyme preparation was frozen in liquid nitrogen and stored at −70°C.

Amino Acid and Metal Content. Five independently purified batches of AlkB were subjected to quantitative amino acid analysis to determine absolute protein concentrations and to metal analysis by inductively coupled plasma atomic emission spectrometry.

AlkB Assay. The activity of AlkB was monitored spectrophotometrically as the octane-dependent rate of NADPH oxidation (4) in the presence of excess recombinant *P. oleovorans* rubredoxin-2 and maize ferredoxin NADPH reductase. One unit of activity is defined as the oxidation of 1 μmol of NADPH per minute at 22°C. Specific activity (units/mg) was calculated using protein concentrations determined by dye-binding assay and adjusted to a value consistent with amino acid analysis using a conversion factor of 0.75 (26). Alternatively, activity was monitored by gas chromatographic separation of substrate (either octane or 1,7-octadiene) and product (either 1-octanol or octene epoxide, respectively) (8). Samples were first brought to 5% (vol/vol) trichloroacetic acid and extracted with 1/10 volume of chloroform. The chloroform–protein emulsion was separated by centrifugation at 13,000 × *g* and the chloroform phase analyzed using a gas chromatograph equipped with a 30 m × 0.25 mm (inner diameter) HP5 column as described (8). Analytes were detected by either flame ionization or total ion detectors and identified by comparison of their fragmentation mass spectra with those of authentic standards.

Scanning Transmission Electron Microscopy. Samples of AlkB were deposited on carbon film as described for the protease ClpP (27). Masses of 480 individual particles were determined with tobacco mosaic virus as a mass standard.

RESULTS

Expression and Purification of AlkB. The *alkB* gene was introduced into *E. coli* under the control of the T7 inducible promoter system. Upon induction, AlkB accumulated to ≈10% of the total protein (Fig. 1*B*). AlkB was purified by differential ultracentrifugation, in which a light membrane fraction was harvested from a 40% glycerol pad, washed with

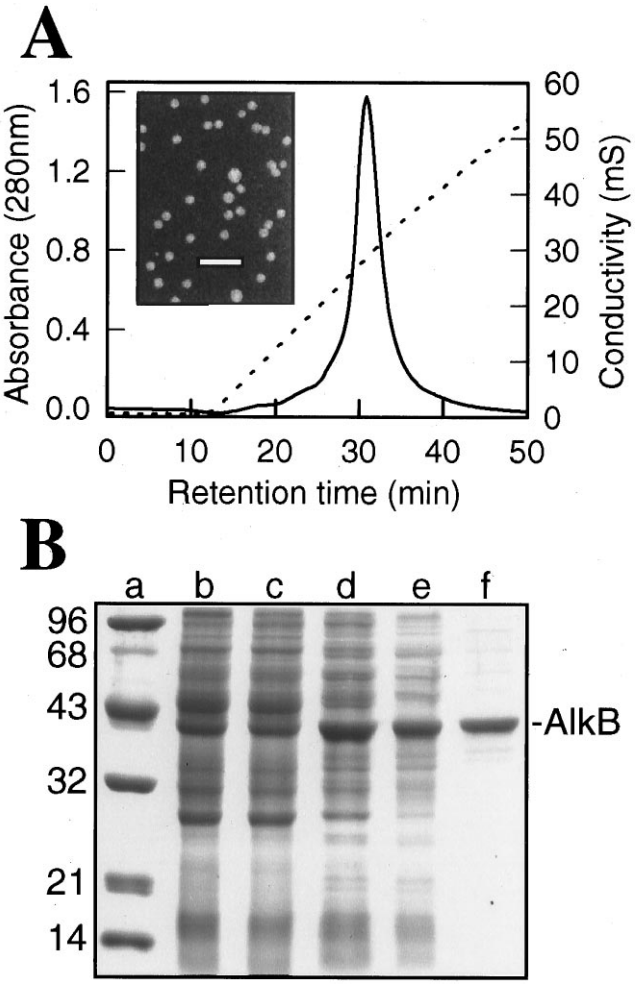

FIG. 1. (*A*) Elution profile from the HPLC carboxymethyl cation exchange column. Solid line, A_{280}; dashed line, conductivity (mS). (*Inset*) Scanning transmission electron micrograph of unstained AlkB particles (bar = 100 nm.) (*B*) Coomassie stained 11% polyacrylamide gel of samples from various stages of purification. Lanes: a, standards; b, total extract of *E. coli* expressing AlkB; c, supernatant of 43,000 × *g* centrifugation; d, glycerol pad; e, urea-washed membranes collected by centrifugation; f, carboxymethyl column eluate collected by ultracentrifugation.

0.5 M urea to remove surface associated proteins, and collected by centrifugation. The resulting pellet was sonicated into a suspension that was applied to an HPLC carboxymethyl cation exchange column. AlkB eluted from this column as a single symmetrical peak (Fig. 1*A*). Scanning transmission electron microscopy analysis of the eluate fractions revealed protein vesicles of 3,680 ± 540 kDa composed of 80 ± 12 AlkB molecules (Fig. 1*A*). Fractions highest in activity were pooled, collected by centrifugation, and resuspended by sonication. The yield of purified AlkB was ≈2 mg/liter of induced cells, and the final purified material was ≈1–2 mM. The samples were judged to be >90% pure based on Coomassie staining, with no single contaminant representing more than ≈2% of the total protein (Fig. 1*B*).

Characterization of the Purified AlkB. AlkB was shown to be catalytically active as judged by octane-dependent consumption of NADPH and by GC analysis of NADPH dependent hydroxylation of octane or epoxidation of 1,7-octadiene. The specific activity of purified AlkB was between 3.6 and 5.2 units/mg, as determined spectrophotometrically. Highly purified AlkB (1–2 mM) was stable to storage and lost no activity during several cycles of freezing in liquid nitrogen or during storage at −70°C for periods of several months. Previous studies of lower specific activity AlkB suggested that there was 1 mol of iron per mol of protein (5). The higher specific activity AlkB reported here has a mean stoichiometry of 3.1 ± 0.2 mol of iron per mol of enzyme, and no other metal was identified in a significant stoichiometric amount.

Optical Spectra. The final preparations contain AlkB in vesicles that strongly scatter the incident light, resulting in a high background absorbance in the visible region. The low molar absorptivity of diiron centers ($\varepsilon_{340} \approx 4$–$5$ $mM^{-1}\cdot cm^{-1}$), along with the lack of definition of such features prevented the identification of charge transfer bands associated with an oxo-bridged diiron center.

Mössbauer Studies. We have studied the Mössbauer spectra of several preparations of AlkB between 4.2 K and 140 K in applied fields up to 8.0 T. These studies have revealed four iron environments: two associated with the sites of a dinuclear cluster (≈60% of Fe), one mononuclear ferrous species (S_A), and a heterogeneous mononuclear high-spin ferric species (S_B). Although the proportions of these species varied, their spectral parameters were essentially the same between preparations.

The 4.2 K Mössbauer spectrum of as-isolated AlkB (Fig. 2*A*) exhibited three quadrupole doublets. The majority species, accounting for ≈60% of the total Fe, consisted of two doublets (doublets 1 and 2) in equal proportions with parameters $\Delta E_Q(1) = 1.70$ mm/s, $\delta(1) = 0.55$ mm/s and $\Delta E_Q(2) = 1.13$ mm/s, $\delta(2) = 0.51$ mm/s. These parameters are in the range observed for exchange-coupled Fe(III)–Fe(III) clusters in diiron enzymes, and most closely match those of toluene-4-monooxygenase (T4MO), which has $\Delta E_Q(1) = 1.55$ mm/s, $\delta(1) = 0.56$ mm/s and $\Delta E_Q(2) = 0.93$ mm/s, $\delta(2) = 0.51$ mm/s (20). The as-isolated AlkB also contained a high-spin ferrous species (S_A) with quadrupole splitting, $\Delta E_Q = 3.2$ mm/s, and isomer shift, $\delta = 1.1$ mm/s (solid line above Fig. 2*A*, ≈20% of the sample Fe), and a high-spin ferric species, the presence and properties of which were best defined by high field measurements. Moreover, the assignment of doublets 1 and 2 to an exchange-coupled Fe(III)–Fe(III) cluster of the type found in diiron proteins demands that these doublets belong to a diamagnetic site, which can also be probed using high field measurements.

The high field Mössbauer spectra of as-isolated AlkB are shown in Fig. 3. The prominent absorption bands at −7 mm/s and +8 mm/s are typical of the magnetic splittings observed for monomeric high-spin Fe(III). This observation is supported by EPR data that showed multiple weak and poorly resolved high-spin Fe(III) signals (from at least three species) between $g \approx 4$ and 9.5. To quantitate the amount of S_B, Mössbauer spectra recorded in strong applied magnetic fields

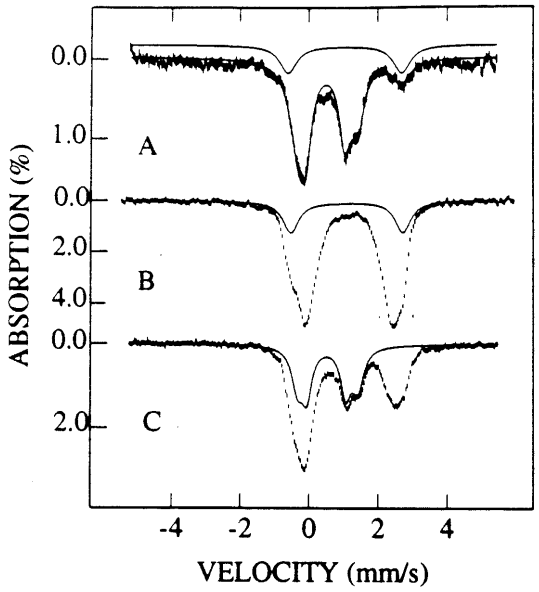

FIG. 2. The 4.2 K Mössbauer spectra of AlkB as-isolated (*A*), reduced by dithionite (*B*), and reoxidized in air in the presence of substrate (*C*). Solid line through the data of *A* is a spectral simulation of three doublets with proportions listed in Table 1; the theoretical spectrum of sites 1 and 2 of the Fe(III)–Fe(III) cluster is shown separately in *C* and that of S_A is drawn above the data of *A* and *B*. The mismatch in intensity in the central part of the spectrum is due to the presence of ferric species S_B. The solid line in *C* shows the contribution of the Fe(III)–Fe(III) cluster (parameters are listed in Table 1). Samples for *A* and for *B* and *C* are from different preparations. The sample of *B* and *C* was obtained by combining AlkB from two preparations to obtain a better signal/noise ratio for studies in strong applied fields; in the as-isolated state, ≈48% of the iron in the combined sample was in the Fe(III)–Fe(III) state; after exposure to air and substrate, 45% of the Fe was found to be Fe(III)–Fe(III).

are particularly useful. For high-spin Fe(III) in octahedral sites with N/O coordination, the zero-field splitting parameter, |D|, is generally smaller than 1.5 cm^{-1}, and the ^{57}Fe magnetic hyperfine coupling constants are, within ± 5%, A ≈ −28 MHz. For such sites, Mössbauer spectra recorded in an applied field of 8.0 T are essentially independent of D, and different high-spin Fe(III) species will exhibit nearly the same high-field spectrum. The spectral simulation shown above Fig. 3*A*, generated with parameters indicated in Table 1, shows that the sample contains ≈20% monomeric high-spin Fe(III).

The central (triplet) feature in the spectrum of Fig. 3*A* belongs to the dinuclear Fe(III)–Fe(III) cluster. Since ferrous S_A also contributes to the central part of the spectrum, the high-field spectrum of the Fe(III)–Fe(III) cluster was prepared by subtracting the spectra from two preparations of AlkB. These preparations had approximately the same ratio of S_A and S_B, but differed in the concentration of the Fe(III)–Fe(III) cluster. By subtracting the spectra, the contributions of S_A and S_B were nearly canceled, and the spectrum of Fig. 3*B* was obtained. The solid line in Fig. 3*B* has been generated under the assumption that the iron sites of doublets 1 and 2 are diamagnetic. The excellent match of the simulation with the observed splittings shows that this assumption is correct, and thus confirms the presence of a dinuclear cluster in AlkB. This simulation also closely matches the spectrum of Fig. 3A, for which the solid line drawn through the data is the sum of the contributions of ferric S_B (≈20%) and the Fe(III)–Fe(III) cluster (≈60%). The remainder of the experimental absorption, in part flanking the features of the Fe(III)–Fe(III) cluster, is due to ferrous S_A. Since the high-field spectrum of S_A depends on seven fine structure and hyperfine parameters, we have made no attempts to simulate it.

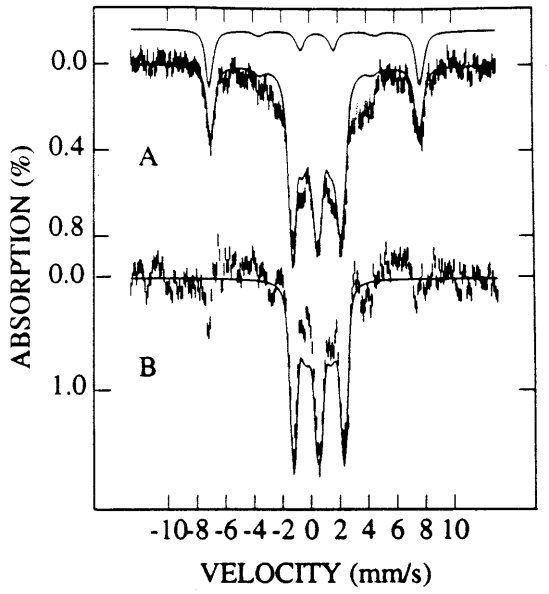

FIG. 3. (*A*) The 4.2 K Mössbauer spectrum of as-isolated AlkB recorded in a magnetic field of 8.0 T applied parallel to the observed γ-radiation. (*B*) The spectrum, which represents the Fe(III)–Fe(III) cluster, was generated as described in the text. The solid line in *B* is a spectrum computed with the assumption that the Fe(III)–Fe(III) cluster is diamagnetic. The solid line through the data in *A* is the sum of spectra computed for S_B (≈20% of total Fe) and the Fe(III)–Fe(III) cluster (≈60%); the contribution of ferrous S_A has not been taken into account. The solid line above the data of *A* represents a simulation of the contribution of S_B (parameters listed in Table 1).

The assignment of doublets 1 and 2 to an exchange-coupled Fe(III)–Fe(III) cluster suggests that reduction should convert these ferric sites to high-spin ferrous cluster sites. In addition, S_B should also be converted to a high-spin ferrous species, while S_A should not be affected. Fig. 2*B* shows a 4.2 K spectrum of reduced AlkB obtained by addition of a 3-fold molar excess of sodium dithionite. This spectrum reflects a mixture of (at least) four high-spin ferrous species with ΔE_Q values ranging from 2.4 to 3.3 mm/s and average $\delta \approx 1.1$ mm/s. Comparison of the spectra of Fig. 2 *A* and *B* shows that all iron of doublets 1 and 2 has been reduced into the high-spin ferrous state. This is consistent with the behavior of protein-bound dinuclear Fe(III)–Fe(III) clusters.

After recording the spectrum of the dithionite-reduced sample of Fig. 2*B* (which contains the contributions of the diferrous cluster, ferrous S_A, and ferrous S_B), the sample was thawed and stirred in air for 10 min. A Mössbauer spectrum recorded after refreezing the sample revealed that none of the iron components had become measurably oxidized by this exposure (data not shown). However, the addition of octane, followed by stirring in air for 10 min, yielded the sample of Fig. 2*C*. Analysis of the 0.05 T and 8.0 T spectra showed that, within ±5%, all of the Fe(II)–Fe(II) cluster had been reoxidized to the Fe(III)–Fe(III) state. In contrast, the iron of S_A and S_B remained essentially in the ferrous state (≈7% of total Fe was observed as monomeric Fe(III) using high field measurements).

To associate the reoxidation of the Fe(II)–Fe(II) cluster with catalytic activity, the reoxidized AlkB sample was analyzed for product formation using GC-mass spectrometry. A retention time and fragmentation pattern consistent with 1-octanol were obtained. Because the AlkB preparation contained high levels of lipids that produced a high background, quantitation of the single turnover yield was precluded. Therefore, the same AlkB sample was next analyzed under steady-state assay conditions. The specific activity determined from the rate of octane-dependent consumption of NADPH was indistinguishable from that determined before the Mössbauer experiment. In addition, because the catalytic samples contained substantially lower levels of lipids, 1-octanol was readily detectable by GC-mass spectrometry. Because only the diiron center was observed to undergo substrate-dependent reoxidation, and because this reaction produced 1-octanol, we conclude that the diiron center occupies the AlkB active site.

Table 1. The 4.2 K Mössbauer parameters of AlkB

Species	Fraction of total Fe*	ΔE_Q, mm/s	δ,† mm/s
Fe(III)–Fe(III)	≈0.6 [0.55–0.62]	1.70 (5)‡	0.55 (3)
		1.13 (5)	0.51 (3)
Fe(II)–Fe(II)		2.4–3.3§	1.05–1.15§
Ferrous S_A	≈0.20 [0.15–0.22]	3.2	1.1
Ferric S_B¶	≈0.20 [0.18–0.22]	0.7	0.5

*Percentages given are for the sample of Figs. 2*A* and 3*A*. Samples from two other preparations had less Fe(III)–Fe(III) (≈35% and 50%). Numbers in square brackets give an estimated range of fractions compatible with our data.
†Quoted relative to Fe metal at 298 K.
‡Numbers in parentheses represent estimated uncertainties in the last significant digit.
§Range of parameters; see comments in the text.
¶Monomeric high-spin Fe(III) of Fig. 3*B*; the magnetic hyperfine tensor used for simulation was A = −(27, 28, 29) MHz, ΔE_Q = 0.7 mm/s, and δ = 0.45 mm/s. The use of an anisotropic A tensor provides the flexibility to account for the possible presence of multiple species with slightly different A values.

To summarize, the predominant iron species in AlkB has properties similar to the clusters of diiron proteins such as hemerythrin (Hr), MMO, T4MO, and Δ9D. AlkB contains an antiferromagnetically coupled pair of high-spin Fe(III) ions in the resting state, the cluster becomes high-spin diferrous upon addition of dithionite, and is quantitatively reoxidized by enzymatic turnover upon the addition of air and substrate. Quantitative protein and metal analysis for the Mössbauer sample of Figs. 2*A* and 3*A* yielded ≈3 Fe per AlkB (Table 1). Because ≈60% of the total iron is associated with the diiron cluster, this sample of AlkB had 0.9 clusters/AlkB. A similar analysis of other preparations yielded slightly lower occupancies of ≥0.65.

Three further conclusions can be drawn from consideration of the spectra in Fig. 2. First, the spectral features of ferrous S_A, drawn separately in Fig. 2 *A* and *B*, differ from those of the Fe(II)–Fe(II) cluster (S_A has a larger δ-value), indicating that S_A in the as-isolated enzyme does not represent a fraction of clusters in the diferrous state. Second, the spectral features of ferrous S_A and S_B also differ, suggesting that ferrous S_A and ferric S_B observed in the as-isolated enzyme represent different sites rather than two redox states of the same iron site. Third, the data of Fig. 2 suggest that the spectrum of the Fe(II)–Fe(II) cluster could be prepared by subtracting the contribution of the Fe(III)–Fe(III) cluster from the data of Fig. 2*C*, followed by subtraction of the resulting representation of ferrous S_A and ferrous S_B from the spectrum of Fig. 2*B*. The spectral features of the ferrous ions in both the cluster and species S_A and S_B did not allow us to obtain a good representation of the spectrum of the Fe(II)–Fe(II) cluster.¶ However, these subtractions indicate that both cluster sites have δ values

¶The doublets of Fe(II)–Fe(II) proteins generally exhibit non-Lorentzian line shapes, reflecting a distribution, not necessarily symmetric, of ΔE_Q and δ values about their means. Similar observations hold for S_A and S_B. These spectra are indicative of iron sites that are sensitive to variations in coordination environments, and their line shapes may change when the samples are thawed and refrozen. We have observed line shape variations of the fully reduced AlkB after exposure to air and refreezing.

between 1.05 mm/s and 1.15 mm/s and quadrupole splittings between 2.4 mm/s and 3.3 mm/s.

A further question related to the structure of diiron clusters in proteins is the nature of the bridging ligands. In addition to one or two bridging carboxylates, the two ferric sites of structurally characterized diiron proteins are linked by either μ-oxo or μ-hydroxo groups. The μ-oxo group provides a strong antiferromagnetic coupling pathway giving rise to exchange coupling constants $>200\ cm^{-1}$ [$J = 216\ cm^{-1}$ for *E. coli* R2 and $J = 268\ cm^{-1}$ for metHr (28); $\mathcal{H}_{ex} = JS_1 \cdot S_2$]. In contrast, the μ-hydroxo bridged cluster of MMO has $J \approx 20\ cm^{-1}$ (19). Thus, J conveys information about the bridging ligands.

It was described elsewhere (20, 23, 29) how the magnitude of J can be assessed from an analysis of Mössbauer spectra recorded in strong applied magnetic fields in the temperature range $4.2\ K \leq T \leq 100\ K$. The shapes of the spectra depend crucially on the relaxation rate of the spin of the Fe(III)–Fe(III) cluster relative to the nuclear precession frequencies. We have recorded 8.0 T spectra of as-isolated AlkB at temperatures between 20 K and 140 K (data not shown). For the analysis of the spectra, we have considered fast, slow, and intermediate relaxation rates. Fast spin-relaxation would cause only small changes in the magnetic splittings as thermally accessible excited spin states become populated and would not allow us to estimate J. Although the relaxation rates of the spins of ferric sites in nonheme proteins are generally not fast for $T < 100\ K$, the presence of S_A and S_B may increase the relaxation rate of the Fe(III)–Fe(III) cluster spin and preclude the determination of J. Therefore, fast relaxation cannot be excluded. In contrast, for slow or intermediate relaxation, spectral changes associated with population of excited states would be readily recognized experimentally.‖ We have observed no spectral changes, within the uncertainties, for $T < 100\ K$, and from spectral simulations we conclude that J must be larger than $80\ cm^{-1}$ if the relaxation is intermediate or slow.

EPR Studies. EPR signals have been reported for the diferric, the mixed-valence, and diferrous states of diiron proteins (28). For the Fe(III)–Fe(III) state, an integer spin EPR signal may be observed if excited spin multiplets are thermally accessible at temperatures for which the spin relaxation rate is sufficiently slow to permit detection of EPR; thermally accessible spin multiplets are associated with a μ-hydroxo bridge, and this resonance has only been reported for MMO (19). Integer spin EPR signals have been observed for the Fe(II)–Fe(II) states of MMO, R2, Hr·N_3 (28), and T4MO (20). R2, Hr, MMO, and uteroferrin also have accessible mixed valence Fe(II)–Fe(III) states and exhibit half integer EPR signals (28, 30, 31).

We have studied a concentrated sample (1.5 mM protein) of as-isolated AlkB with EPR, in parallel and perpendicular mode, between 10 K and 100 K; no resonance attributable to the diferric cluster was observed. The absence of an integer spin EPR signal does not prove but is consistent with the conclusion that $J > 80\ cm^{-1}$. For samples of AlkB in the as-isolated and fully reduced forms, we did not observe any EPR signal indicative of a mixed-valence state.

DISCUSSION

AlkB belongs to a class of non-heme-iron containing integral-membrane enzymes that includes hydroxylases and fatty acid desaturases (12). Expression of AlkB described here results in the accumulation of substantial amounts of catalytically active enzyme. Our initial purification attempts included detergent solubilization, as recently described by Peters and Witholt (32). However, these preparations lost activity within a few hours. Since earlier purifications used diethylaminoethyl cellulose, we screened additional chromatographic media and found that AlkB could be highly enriched by separation on carboxymethyl HPLC media. Surprisingly, when membrane fractions obtained by differential centrifugation were applied to this medium, AlkB eluted as a sharp peak composed of nearly homogeneous protein that could be concentrated to unusually high levels (50–100 mg/ml); this behavior is more reminiscent of a soluble than an integral-membrane protein. Electron microscopy revealed regular vesicular structures consisting of ≈80 AlkB monomers, suggesting that some structural feature of AlkB favors self-association from which other proteins are excluded. AlkB thus prepared has the highest specific activity reported to date (up to 5.2 units/mg), is stable at 4°C, and is resistant to freeze-thaw cycles.

We have provided evidence that AlkB contains a dinuclear iron cluster with spectroscopic properties similar to the clusters found in diiron proteins and enzymes, including those that catalyze O_2-dependent hydrocarbon oxidations (17, 19–21, 23, 28). In the as-isolated state, the cluster contains an antiferromagnetically coupled pair of high-spin Fe(III) ions. The observation of two distinct quadrupole doublets in this state implies different coordination environments for the two iron sites. As described above, the exchange coupling constant J conveys information regarding the nature of the bridging ligands. Because of the presence of species S_A (≈20% of Fe) and S_B (≈20%) and because of the unknown relaxation rates of the cluster spin, we could not establish a precise lower limit for the value of J. However, if the relaxation rate of the electronic spin of the cluster is slow or intermediate on the Mössbauer time scale (≈10 MHz), as is commonly the case for high-spin Fe(III) in proteins, our analysis indicates that $J > 80\ cm^{-1}$. This tentative conclusion is also supported by the lack of broadening of the zero field Mössbauer spectra at temperatures up to 200 K and by the absence of an integer spin EPR signal associated with the diferric cluster. Thus, while our preliminary analysis is consistent with the presence of an oxo-bridge, a determination of a lower bound for J is required before definite conclusions can be drawn.

The mononuclear species S_A and S_B were present in variable amounts, ranging between 0.55–0.93 S_A and 0.45–0.80 S_B per AlkB. The EPR and Mössbauer properties of S_B suggest that this species represents iron contained in one heterogeneous site or adventitiously bound iron in different sites. It is also possible that S_A may comprise several species, since high-spin ferrous sites with different octahedral N/O coordination exhibit similar zero field Mössbauer spectra. Because attempts to remove S_A and S_B by chelators were unsuccessful, we have considered whether these species have a role in AlkB catalysis. A 10-min exposure of reduced AlkB to air caused no measurable reoxidation of the dinuclear center, S_A, or S_B. In contrast, the dinuclear center alone was quantitatively oxidized in the presence of air and substrate (octane), while S_A and S_B were again nonreactive. This single turnover reoxidation, coupled with the production of 1-octanol, thus provides compelling evidence that the diiron center resides in the AlkB active site. The insensitivity of reduced AlkB to air in the absence of substrates is similar to the behavior of Δ9D (18). Thus, at least for two diiron enzymes, the active site structure conserves reducing equivalents in the absence of substrate. Finally, the Mössbauer spectrum of Fig. 2*C* reveals that electron transfer does not occur between the diferric cluster and ferrous S_A and S_B. Further experiments are required to determine whether S_A

‖The zero field spectra of MMO ($J \approx 20\ cm^{-1}$), T4MO ($J \approx 20$–$40\ cm^{-1}$), and uteroferrin ($J \geq 80\ cm^{-1}$) exhibit considerable line broadening at temperatures for which excited state multiplets are populated. The cause of this broadening is not well understood. It may arise when the relaxation processes involve pairs of levels of excited multiplets so closely spaced that magnetic ^{57}Fe hyperfine interactions can mix the electronic states. This mixing could produce magnetic features in the zero field spectra of the integer spin system. The zero-field spectra of AlkB do not exhibit any broadening up to 200 K, which supports our suggestion that J is $\geq 80\ cm^{-1}$.

and S_B represent adventitiously bound iron or whether either site perhaps serves a structural function.**

As observed for other diiron proteins, the AlkB cluster is reduced to a diferrous state containing high-spin sites upon addition of dithionite. Due to the presence of ferrous species S_A and S_B in the reduced enzyme, we could only establish ranges for the isomer shifts and quadrupole splittings of the two ferrous sites. The range quoted for ΔE_Q is consistent with protein-bound diiron clusters, while the isomer shift, $1.05 \leq \delta \leq 1.15$ mm/s, is smaller than the values reported for most protein-bound clusters (1.20–1.30 mm/s). The coordination environments of MMO, R2, and Δ9D ($FeNO_{3-5}$) produce shifts ≥1.25 mm/s, while deoxyHr (FeN_3O_3 and FeN_2O_3 sites) exhibits δ of 1.14 mm/s (35). The smaller shifts estimated for diferrous AlkB suggest a cluster environment rich in nitrogen-coordinating ligands.

AlkB contains the eight-histidine motif common to nonheme integral-membrane desaturases and hydroxylases. In the rat desaturase, these eight His are essential for catalysis (12). In this context, it is interesting to note that the Mössbauer parameters of diferrous AlkB would be consistent with multiple His ligands. A recent search of the ≈10^6 primary sequences in GenBank (version 65) revealed 75 proteins of known function containing the eight-histidine motif [$HX_{3-4}HX_{7-41}$(3 non-His)HX_{2-3}(1 non-His)HHX_{61-189}(40 non-His)HX_{2-3}(1 non-His)HH]. These matches include 66 integral-membrane enzymes and 9 soluble proteins. All of the 66 integral-membrane enzymes catalyze O_2-dependent modifications of hydrocarbon substrates and represent at least 11 distinct activities: 5 desaturases [4 fatty acid, 1 steroid (36)]; 3 hydroxylases (fatty acid, xylene, and alkane); 2 oxidases [C-4 sterol methyl (36) and carotene]; and 1 decarbonylase [aldehyde (37)]. Thus, we reason that these membrane enzymes may share a common catalytic core that is associated with the presence of the eight-histidine motif. Moreover, based on the Mössbauer properties of AlkB, we propose that this entire class of enzymes also contains some variation of an active site diiron cluster. If this proposal is correct, there would be two major classes of enzymes containing diiron centers that are used for O_2-activation, one soluble and one integral membrane, each with its own distinct consensus motif. The presence of diiron clusters in both soluble and membrane protein families would greatly extend the role of diiron centers in O_2-activation biochemistry, which may perhaps rival the functional versatility of the P450 enzymes.

We thank Dr. E. Cahoon for assistance with gas chromatography-MS, E. Whittle for technical assistance, Dr. J. Wall and Dr. M. Simon for assistance with the scanning transmission electron microscopic analysis, M. Giles and Dr. A. J. Francis for assistance with the ICP-AES analysis, and J. Leykam (Michigan State University) for the quantitative amino acid analysis. This work was supported by a grant from the U.S. Department of Energy Office of Basic Energy Sciences to J.S. and grants from the National Institutes of Health to E.M. (Grant GM-22701) and to B.G.F. (Grant GM-50853). B.G.F. is a Searle Scholar of the Chicago Community Trust (1994–1997) and a Shaw Scientist of the Milwaukee Foundation (1994–1999).

1. Peterson, J. A., Basu, D. & Coon, M. J. (1966) *J. Biol. Chem.* **241,** 5162–5164.
2. Ueda, T. & Coon, M. J. (1972) *J. Biol. Chem.* **247,** 5010–5016.
3. Peterson, J. A., Kusunose, M., Kusunose, E. & Coon, M. J. (1967) *J. Biol. Chem.* **242,** 4334–4340.
4. McKenna, E. J. & Coon, M. J. (1970) *J. Biol. Chem.* **245,** 3882–2889.
5. Ruettinger, R. T., Griffith, G. R. & Coon, M. J. (1977) *Arch. Biochem. Biophys.* **183,** 528–537.
6. Kok, M., Oldenhuis, R., van der Linden, M. P. G., Ratjees, P., Kingma, J., van Lelyveld, P. H. & Witholt, B. (1989) *J. Biol. Chem.* **264,** 5435–5441.
7. Katopodis, A. G., Smith, H. T., Jr., & May, S. W. (1988) *J. Am. Chem. Soc.* **110,** 897–899.
8. Colbert, J. E., Katopodis, A. G. & May, S. W. (1990) *J. Am. Chem. Soc.* **112,** 3993–3996.
9. Fu, H., Newcomb, M. & Wong, C.-H. (1991) *J. Am. Chem. Soc.* **113,** 5878–5880.
10. Guengerich, F. P. (1992) *FASEB J.* **6,** 667–668.
11. Lipscomb, J. D. (1994) *Annu. Rev. Microbiol.* **48,** 371–399.
12. Shanklin, J., Whittle, E. & Fox, B. G. (1994) *Biochemistry* **33,** 12787–12794.
13. van Beilen, J. B., Penninga, D. & Witholt, B. (1992) *J. Biol. Chem.* **267,** 9194–9201.
14. Nordlund, P. & Eklund, H. (1993) *J. Mol. Biol.* **232,** 123–164.
15. Rosenzweig, A. C., Nordlund, P., Takahara, P. M., Frederick, C. A. & Lippard, S. J. (1995) *Chem. Biol.* **2,** 409–418.
16. Lindqvist, Y., Huang, W., Schneider, G. & Shanklin, J. (1996) *EMBO J.* **15,** 4081–4092.
17. Fox, B. G., Shanklin, J., Somerville, C. & Münck, E. (1993) *Proc. Natl. Acad. Sci. USA* **90,** 2486–2490.
18. Fox, B. G., Shanklin, J., Ai, J., Loehr, T. M. & Sanders-Loehr, J. (1994) *Biochemistry* **33,** 12776–12786.
19. Fox, B. G., Hendrich, M. P., Surerus, K. K., Andersson, K. K., Froland, W. A., Lipscomb, J. D. & Münck, E. (1993) *J. Am. Chem. Soc.* **115,** 3688–3701.
20. Pikus, J. D., Studts, J. M., Achim, C., Kauffmann, K. E., Münck, E., Steffan, R. J., McClay, K. & Fox, B. G. (1996) *Biochemistry* **35,** 9106–9119.
21. Liu, K. E., Valentine, A. M., Wang, D., Huynh, B. H., Edmondson, D. E., Salifoglou, A. & Lippard, S. J. (1995) *J. Am. Chem. Soc.* **117,** 10174–10185.
22. Gupta, N., Bonomi, F., Kurtz, D. M., Jr., Ravi, N., Wang, D. L. & Huynh, B. H. (1995) *Biochemistry* **34,** 3310–3318.
23. Sage, J. T., Xia, Y.-M., Debrunner, P. G., Keough, D. T., de Jersey, J. & Zerner, B. (1989) *J. Am. Chem. Soc.* **111,** 7239–7247.
24. Fox, B. G., Froland, W. A., Jollie, D. R. & Lipscomb, J. D. (1990) *Methods Enzymol.* **188,** 191–202.
25. Rosenberg, A. H., Lade, B. N., Chui, D.-S., Lin, S.-W., Dunn, J. J. & Studier, F. W. (1987) *Gene* **56,** 125–135.
26. Gogstad, G. O. & Krutnes, M. (1982) *Anal. Biochem.* **126,** 355–359.
27. Flanagan, J. M., Wall, J. S., Capel, M. S., Schneider, D. K. & Shanklin, J. (1995) *Biochemistry* **34,** 10910–10917.
28. Que, L., Jr., & True, A. E. (1990) in *Dinuclear Iron- and Manganese-Oxo Sites in Biology*, ed. Lippard, S. J. (Wiley, New York), Vol. 38, pp. 97–200.
29. Zang, Y., Dong, Y., Que, L., Jr., Kauffmann, K. & Münck, E. (1995) *J. Am. Chem. Soc.* **117,** 1169–1170.
30. Hendrich, M. P., Elgren, T. E. & Que, L., Jr. (1991) *Biochem. Biophys. Res. Commun.* **176,** 705–710.
31. Atta, M., Debaecke, N., Andersson, K. K., Latour, J.-M., Thelander, L. & Gräslund, A. (1996) *J. Biol. Inorg. Chem.* **1,** 210–220.
32. Peters, J. & Witholt, B. (1994) *Biochim. Biophys. Acta* **1196,** 145–153.
33. Stassinopoulos, A., Schulte, G., Papaefthymiou, G. C. & Caradonna, J. P. (1991) *J. Am. Chem. Soc.* **113,** 8686–8697.
34. Que, L., Jr., & Dong, Y. (1996) *Acc. Chem. Res.* **29,** 190–196.
35. Kurtz, D. M., Jr. (1990) *Chem. Rev.* **90,** 585–606.
36. Bard, M., Bruner, D. A., Pierson, C. A., Lees, N. D., Biermann, B., Frye, L., Koegel, C. & Barbuch, R. (1996) *Proc. Natl. Acad. Sci. USA* **93,** 186–190.
37. Aarts, M. G., Keijzer, C. J., Stiekema, W. J. & Pereira, A. (1995) *Plant Cell* **7,** 2115–2127.

**It is formally possible that S_A might be linked to the dinuclear center to form a trinuclear cluster. Due to the complexity of the spectra, a 1:1 stoichiometry of S_A and Fe(III)–Fe(III) cannot be strictly ruled out. However, the range of fractions given in Table 1 suggests that the amount of S_A iron is too small to form a {S_A Fe(III)–Fe(III)} cluster. We can also consider the problem from a standpoint of exchange interactions. Assume a dinuclear cluster antiferromagnetically coupled by $J\boldsymbol{S_1}\cdot\boldsymbol{S_2}$ and assume that a ferrous ion, with spin $\boldsymbol{S_3}$, is coupled to cluster site 1 by $j_{13}\boldsymbol{S_1}\cdot\boldsymbol{S_3}$. The j_{13} term induces internal fields, H_{int}, at the ^{57}Fe nuclei of sites 1 and 2 of the cluster given, in first order perturbation, by $|H_{int}(1,2)| = (35\sqrt{2}/6)|(j_{13}/J)(A^{III}/g_n\beta_n)|$, where $A^{III}/g_n\beta_n \approx -20$ T for a ferric site with N/O coordination. Our data show that $|H_{int}(1,2)| < 0.1$ T, implying that $|j_{13}/J| < 0.001$. This suggests that $|j_{13}|$ is of order 0.1 cm^{-1}, an unusually small coupling for a ferric-ferrous pair (28). For the case that $\boldsymbol{S_3}$ would be coupled to both iron sites of the dinuclear cluster, $j_{13}\boldsymbol{S_1}\cdot\boldsymbol{S_3} + j_{23}\boldsymbol{S_2}\cdot\boldsymbol{S_3}$, our data imply that $|\Delta j| = |j_{13} - j_{23}| < 0.1$ cm^{-1}. Given that the two ferric sites of the dinuclear cluster have different ligand environments as indicated by their distinct ΔE_Q values, a $|\Delta j/J| \leq 0.001$ is rather improbable. Finally, we note that the reaction catalyzed by AlkB requires oxygen activation chemistry of the type catalyzed by both diiron enzymes (11) and synthetic dinuclear iron complexes (33, 34).